Characterization and Inhibition of the Main Protease of Severe Acute Respiratory Syndrome Coronavirus

Chih-Jung Kuo[1],*, Po-Huang Liang[2],*

Abstract

The main protease of SARS-associated coronavirus (SARS-CoV), also called 3C-like protease (3CL^{pro}), is vital for the viral replication. It cleaves the replicase polyproteins at 11 sites and is a promising drug target. Several groups of inhibitors have been identified through high-throughput screening and rational drug design. In addition to the pharmaceutical applications, a mutant 3CL^{pro} (T25G) with an expanded S1′ space has been demonstrated to tolerate larger residues at P1′, facilitating the cleavage behind the recognition sequence. This review summarizes current developments in anti-SARS agents targeting 3CL^{pro} and the application of the mutant protease as a tag-cleavage endopeptidase.

Keywords: Coronavirus, Enzymatic hydrolysis, Protease, Protein engineering, Proteins

Received: November 07, 2014; *revised:* January 04, 2015; *accepted:* January 09, 2014

DOI: 10.1002/cben.201400031

1 Introduction

Respiratory viral infective diseases are renowned as a major threat to all ages worldwide, particularly children under 5 years of age [1]. Beginning in late 2002, a severe epidemic disease called severe acute respiratory syndrome (SARS) emerged in China and quickly spread to more than 30 countries and areas [2], causing a significant impact on health and economy. SARS-associated coronavirus (SARS-CoV) typically causes respiratory and enteric diseases, pneumonia, exacerbation of asthma, neurological symptoms, and myocarditis in humans [3–5], with a mortality rate as high as nearly 10 % of those diagnosed [6]. SARS-CoV is a positive-stranded RNA virus belonging to a family of enveloped coronaviruses [5, 7]. The SARS-CoV genome contains five major open reading frames (ORFs) that encode the replicase polyprotein, the spike (S), envelope (E), membrane glycoproteins (M), and the nucleocapsid protein (N). Extensive proteolytic processing of these nonstructural and structural polyproteins is a vital step for providing the functional proteins for SARS-CoV viral propagation, and such processing is mediated primarily by the nonstructural protein 5 (nsp5), the main protease (M^{pro}) with a dimeric chymotrypsin-fold, also known as 3C-like protease (3CL^{pro}) because of its analogy with the monomeric 3C protease (3C^{pro}) form picornavirus [8–10].

In contrast to the common serine proteases containing a Ser-His-Asp catalytic triad, SARS-CoV 3CL^{pro} employs a Cys-His catalytic dyad (Cys145 and His41) in the catalytic site. This is similar to the porcine transmissible gastroenteritis virus (TGEV) 3CL^{pro} and the human coronavirus 229E 3CL^{pro} (HCoV 229E) using Cys144 and His41 [8]. According to the previous studies on the substrate specificities and proteolytic sites, SARS-CoV 3CL^{pro} utilizes the substrates with bulky hydrophobic residues (mainly Leu or Ile), invariable glutamine residue, and small aliphatic residues (Ser, Ala, or Gly) at the P2, P1 and P1′ positions, respectively [8–13]. In addition, secondary structural studies for substrates of SARS-CoV 3CL^{pro} have revealed that substrates with more beta-sheet like structures tend to be cleaved more quickly [12]. The determination of the crystal structures for HCoV 229E 3CL^{pro} and the inhibitor complex of TGEV 3CL^{pro} also confirmed a remarkable degree of conservation of the substrate binding sites for CoV 3CL^{pro} [8].

2 Characterization of SARS-CoV 3CL^{pro}

2.1 Activity Measurements of SARS-CoV 3CL^{pro}

SARS-CoV 3CL^{pro} cleaves pp1a (486 kDa) and pp1ab (790 kDa) polyproteins at the predicted 11 conserved sites (Fig. 1a) with a conserved sequence of (Leu, Met, or Phe)-Gln-(Ser, Ala, or Gly), where the glutamine residue is invariable at the P1 position (Fig. 1b) [12]. The reverse-phase high-pressure liquid chromatography (RP-HPLC) experimental system was used to analyze cleaved products by a linear gradient of aceto-

[1] Prof. Chih-Jung Kuo (corresponding author)
National Chung Hsing University, College of Veterinary Medicine, Department of Veterinary Medicine, Taichung 402, Taiwan.
E-Mail: ck476@nchu.edu.tw

[2] Prof. Po-Huang Liang (corresponding author)
Institute of Biological Chemistry, Academia Sinica, Taipei 115, Taiwan
E-Mail: phliang@gate.sinica.edu.tw

a)

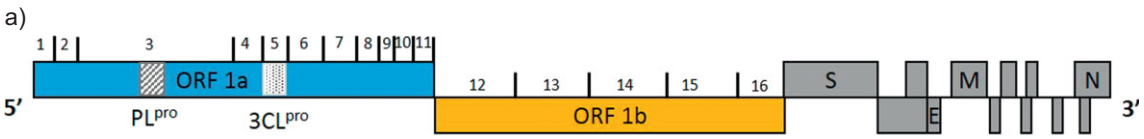

b)

	P6	P5	P4	P3	P2	P1	P1'	P2'	P3'	P4'	
nsp1	R	E	L	N	G	G^{180}	A	V	T	R	PL^{pro} cleavage sites
nsp2	F	R	L	K	G	G^{818}	A	P	I	K	
nsp3	I	S	L	K	G	G^{2740}	K	I	V	S	
nsp4	T	S	A	V	L	Q^{3240}	S	G	F	R	3CL^{pro} cleavage sites
nsp5	S	G	V	T	F	Q^{3546}	G	K	F	K	
nsp6	K	V	A	T	V	Q^{3836}	S	K	M	S	
nsp7	N	R	A	T	L	Q^{3919}	A	I	A	S	
nsp8	S	A	V	K	L	Q^{4117}	N	N	E	L	
nsp9	A	T	V	R	L	Q^{4230}	A	G	N	A	
nsp10	R	E	P	L	M	Q^{4369}	S	A	D	A	
nsp11	P	H	T	V	L	Q^{5301}	A	V	G	A	
nsp12	R	N	V	A	T	Q^{5902}	A	E	N	V	
nsp13	T	F	T	R	L	Q^{6429}	S	L	E	N	
nsp14	F	Y	P	K	L	Q^{6775}	A	S	Q	A	

Figure 1. Schematic diagram of the SARS-CoV polyproteins, with cleavage sites of the two proteases, papain-like protease (PL^{pro}) and 3C-like protease (3CL^{pro}). Numbers 1–16 represent the nonstructural proteins (nsp) 1–16. (a) The SARS-CoV genome encodes four structural proteins: spike (S), envelope (E), matrix (M), and nucleocapsid (N). (b) The cleavage sites and conserved amino acid sequences of PL^{pro} and 3CL^{pro} aligned.

nitrile-containing trifluoroacetic acid (TFA) and to screen inhibitors, but it is a time-consuming process. A fluorogenic substrate, Dabcyl-KTSAVLQSGFRKME-Edans, with the fluorescence quenching pair (Edans-Dabcyl) has been developed to facilitate enzyme assay and inhibitor screening (Fig. 2) [14]. With this or other quenching pairs, such as 2-amino benzoyl-(Abz)-Tyr(NO_2) [15], an intense increase of fluorescence was detectable upon the peptide cleavage by the protease due to the effect of fluorescence resonance energy transfer (FRET). Accompanying a fluorescence plate reader, such a fluorogenic substrate can be applied to high-throughput inhibitor screening. In addition, fluorogenic peptides containing a SARS-CoV 3CL^{pro} consensus cleavage sequence and Rhodamine 110 [(Ala-Arg-Leu-Gln-NH)$_2$-Rhodamine] can also serve as substrates for the enzyme activity assay with high sensitivity (at low pM range) [16].

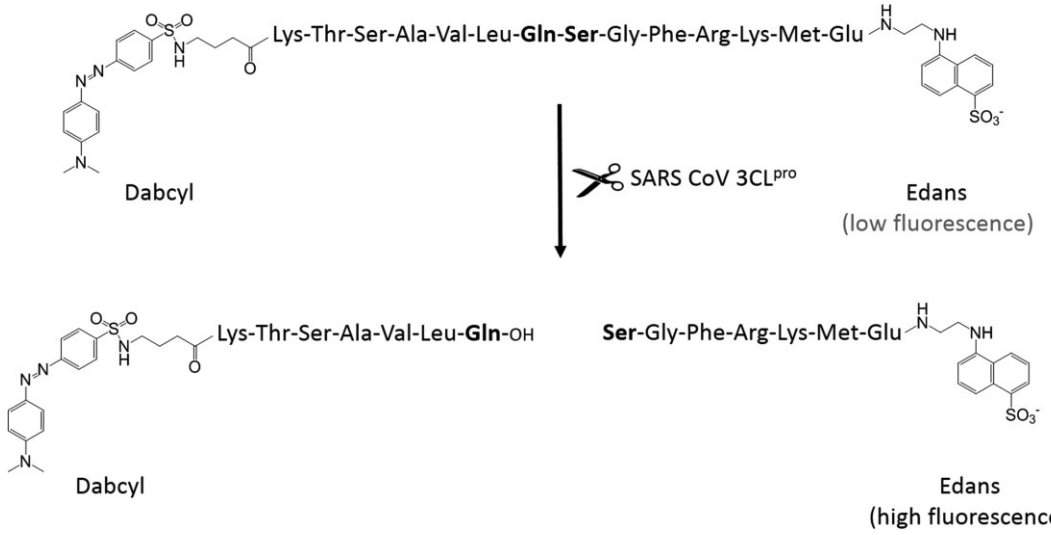

Figure 2. The fluorogenic substrate used for the SARS-CoV 3CL^{pro} inhibition assay. Enhanced fluorescence caused by cleavage of the fluorogenic substrate peptide can be monitored at 538 nm with excitation at 355 nm.

2.2 Dimerization of SARS-CoV 3CL^{pro}

The protease contains three domains (I, II, and III) and the active site is located between domain I and II. The crystal structures of the 3CL^{pro} from TGEV, HCoV 229E, and SARS-CoV [8, 10, 17, 18] reveal a common feature for CoV 3CL^{pro} with two chymotrypsin-like β-domains (domain I & II) and one α-helical dimerization domain (domain III) which is absent from the picornavirus 3C^{pro} and chymotrypsin [19]. In addition, deletion of the first four amino acids in the N terminus significantly increased the dimer dissociation constant (K_D) and accordingly decreased the protease activity [20–21]. From analytic ultracentrifugation (AUC) analysis, sequential deletions of the first 3, 4, and 7 residues at the N terminus caused a 12-, 205-, and 1275-fold increase in dimer K_D, respectively [20], indicating the role of Arg4 in dimerization. Besides the N terminus, a cluster of conserved serine residues (Ser139, Ser144, and Ser147) located adjacent to the active site, but away from the dimer interface of the protease initiates long-range cooperative interactions to modulate dimerization [22]. The mutation of Ser147 to Ala, which does not make any contact with the opposite subunit, totally abolished dimerization and enzyme activity. However, the measured K_D values of the dimer varied [14, 20, 23, 24], but a His-tag of the recombinant protein for NiNTA purification might interfere with the dimer formation [12].

3 Structure of SARS-CoV 3CL^{pro}

From the crystal structure, the N-terminal residues 1–7 (N-finger) are buried in the dimer interface with numerous contacts with the domain II close to the active site of the other protomer (Fig. 3) [10, 18, 25, 26]. The first crystal structure of SARS-CoV 3CL^{pro} is complexed with a substrate-like hexapeptidyl chloromethylketone (Cbz-Val-Asn-Ser-Thr-Leu-Gln-CMK) inhibitor, revealing the structural features of this protease [10]. The protease forms a dimer with two protomers oriented almost at right angles to each other. The Cys-His catalytic dyad is located in an active site cleft between domains I and II, which adopt antiparallel β-barrel structures. Domain III, for mediating the tight dimerization, contains five α-helices arranged into a large antiparallel globular cluster. Another structure of the protease with C-terminal six amino acids from the neighboring protomer bound in the active site (product-bound form) reveals the detailed interactions of the protease with the P1 to P6 amino acids (QFTVGS) [18]. In this structure, two protomers (A and B) form a dimer, and the N terminus of protomer A is located

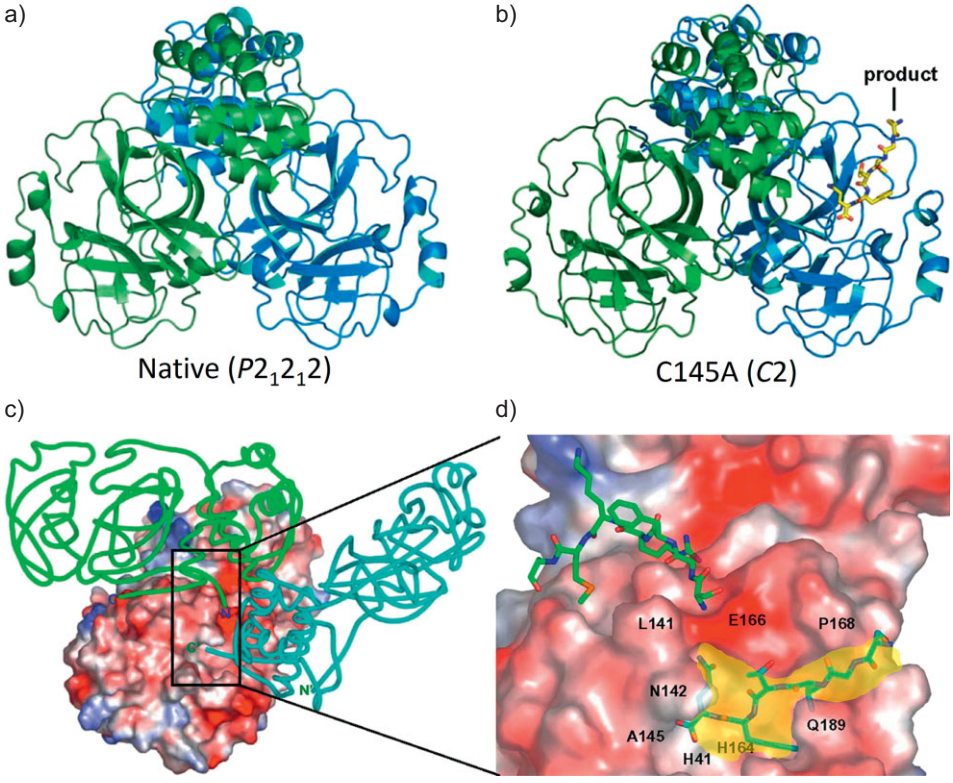

Figure 3. Crystal structures of the wild-type and C145A mutant 3CL^{pro}. In (a) and (b), the overall three-dimensional structures of wild-type (PDB ID 1Z1I) and C145A mutant (PDB ID 1Z1J) 3CL^{pro} are shown as ribbons (protomer A is green and protomer B is blue), and the product in the active site cleft between domain I and II is shown in yellow. (c) The dimer structure is composed of protomer A (shown with a solid tube in green) and protomer B (shown with charge potentials). The C terminus of protomer B′ (shown in cyan) in another asymmetric unit that is intercalated into the active site of protomer B. (d) An enlarged view of (c) near the active site, showing the C-terminal amino acids of protomer B′ as well as the N-terminal amino acids of protomer A in the neighborhood of the active site of protomer B. The active site of protomer B is shown in light yellow.

close to the active site of protomer B. However, in the active site of protomer B, extra electron density originating from the six C-terminal amino acids of protomer B′ (the nearby protomer in the crystal packing) was found. The side chain of Gln (the last C-terminal residue of protomer B′) is ~10 Å away from the side chain of Ser (the first N-terminal residue of protomer A), suggesting a positional shift after autocatalytic cleavage of the premature protease. This structure provides the necessary information for rational design of the active-site inhibitors [18]. The detailed interactions in the active site are as follows. In the S1 site, the side chain Oε1 and Nε2 of Gln306 (P1) form hydrogen bonds with Nε2 of the His163 imidazole ring and the carboxylate of Glu166. The oxygen atom of the side chain of P1-Gln forms H-bonds with the backbone NH atoms of Gly143 and Cys145. Therefore, the Sγ atom of Cys145 is at a suitable position to attack the peptide bond. The S2 site is formed by the main-chain atoms of Val186, Asp187, Arg188, and Gln189 as well as the side chain atoms of His41, Met49, and Met165 to hold a bulky side chain, such as Val, Leu, or Phe at the P2 position. The N atom in the main chain of P2-Phe interacts with the O atom of His164 and the side chain interacts with Met49, Met165, Asp187, and Arg188 through hydrophobic interactions. The side chain of P3-Thr is oriented toward the bulk solvent, so a hydrophilic residue can also exist at this position. The main-chain O atom of P4-Val accepts a H-bond (3.1 Å) from the Nε2 atom of Gln189, and the N atom of the Val donates a H-bond to the Oε1 atom of Gln189, while another main-chain NH donates a H-bond (3.3 Å) to Gln189. The side chain of P4-Val interacts with Met165 and Gln189 via hydrophobic interactions. S5 subsite is composed of the main-chain atoms of Thr190, Ala191, and Gln192. P5-Gly is not in contact with the protease. The S6 site is almost positioned at the outer area of the protein. However, the O atom and Oγ of P6-Ser still interact with the backbone N and O atoms of Gln192.

4 Inhibitors of SARS-CoV 3CL^{pro}

The 3CL^{pro} is essential for the propagation of the virus and, thus, serves as a promising target for anti-SARS therapy. Many inhibitors with micromolar and submicromolar inhibition constants against the SARS-CoV 3CL^{pro} have been identified from the high-throughput random screening using protease activity assays and cell-based assays, or the rational inhibitor design based on known inhibitors, active-site directed approaches targeting the cysteine residue, and structure-based virtual screening, as described below.

4.1 From High-Throughput Screening

Several inhibitors against SARS-CoV 3CL^{pro} identified by different laboratories using high-throughput screening have been described previously [27]. Wu et al. identified ~50 active compounds by cell-based assay that block SARS-CoV replication, including two existing drugs, reserpine and aescin [28]. In the subsequent target verification, a compound named TL-3 that was developed as a transition-state analogue of the HIV protease (inhibition constant K_i = 1.5 nM and 4 nM, against HIV protease and feline immunodeficiency virus protease, respectively) [29] was able to inhibit the SARS-CoV 3CL^{pro} (K_i = 0.6 μM; measured by the Edans-Dabcyl FRET assay) (**1**, Fig. 4). Lopinavir (one of the two components from the anti-AIDS drug Kaletra® from Abbott) was shown to weakly inhibit the protease (K_i = 15 μM), consistent with observed better clinical outcome for treating SARS patients with this drug in a Hong Kong Hospital [30]. Blanchard et al. had screened 50 000 drug-like small molecules to find five novel SARS-CoV 3CL^{pro} inhibitors, MAC-5576, MAC-8120, MAC-13985, MAC-22272, and MAC-30731 (**2**–**6**, Fig. 4), with IC_{50} values of 0.5–7 μM measured using Abz-Tyr(NO_2) FRET assay [15]. Kao et al. screened 50 240 structurally diverse small molecules and found 2 compounds targeting the SARS-CoV 3CL^{pro} [31]. One of the compounds, MP576 (**7**, Fig. 4), a 3-quinolinecarboxylic acid, displayed inhibitory activity with a K_i value of 2.5 μM in the HPLC-based cleavage assay and an EC_{50} value (half maximal effective concentration) of 7 μM in the Vero cell-based SARS-CoV plaque reduction assay without apparent toxicity (CC_{50} (half maximal cytostatic concentration) > 50 μM) [32]. The other compound, MP521 (**8**, Fig. 4), an imidazolidine, exhibited a K_i value of 11 μM, an EC_{50} value of 14 μM, and a CC_{50} value > 50 μM. A library of 960 commercially available drugs and biologically active substances were screened by Hsu et al. using the cell-based assay to find three inhibitors, namely phenylmercuric acetate, thimerosal, and hexachlorophene (**9**–**11**, Fig. 4), which inhibited SARS protease activity according to the Edans-Dabcyl FRET assay [33]. The K_i values of phenylmercuric acetate, thimerosal, and hexachlorophene were determined to be 0.7, 2.4, and 13.7 μM, respectively. Phenylmercuric acetate and thimerosal containing mercury are used as pharmaceutical excipients and more widely used as antimicrobial preservatives in parenteral and topical pharmaceutical formulations [34]. As shown below, other metal-containing compounds (such as zinc-containing compounds) were also identified to be the protease inhibitors. The hexachlorophene derivatives were further explored as SARS-CoV 3CL^{pro} inhibitors with similar inhibitory activity using the Abz-Dnp FRET assay by Liu et al. [35]. Chen et al. screened from a natural product library consisting of 720 compounds to obtain two compounds, tannic acid (IC_{50} (half maximal inhibitory concentration) = 3 μM) and 3-isotheaflavin-3-gallate (TF2B) (IC_{50} = 7 μM), to be inhibitors of SARS-CoV 3CL^{pro} with the Edans-Dabcyl assay [36]. These two large compounds (structures not shown) belong to a group of natural polyphenols in tea [37]. Also from a natural product library, an esculetin-4-carboxylic acid ethyl ester (MC8; **12**, Fig. 4) with an IC_{50} value of 46 μM against SARS-CoV 3CL^{pro} was derived from the marine sponge Axinella corrugate [38]. The screening was performed by using a sensitive red-shifted internally quenched fluorogenic substrate for SARS-CoV 3CL^{pro}, also based on the FRET between the CAL Fluor Red 610 and Black Hole Quencher-1 as a donor-acceptor pair. In the cell-based assays, MC8 is an effective inhibitor of SARS-CoV replication in Vero cells at non-cytotoxic concentrations (EC_{50} = 112 μM; CC_{50} > 800 μM).

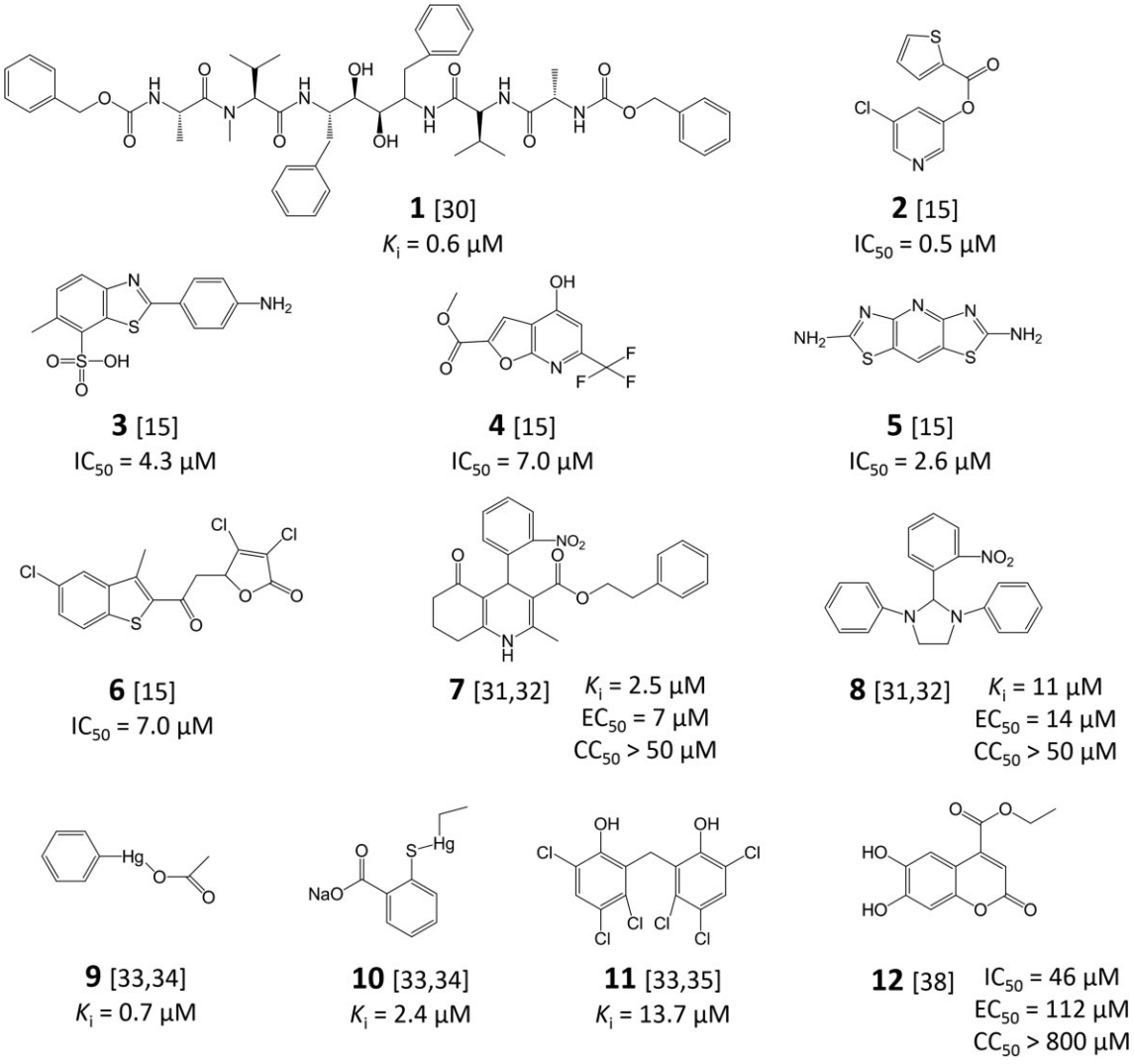

Figure 4. SARS-CoV $3CL^{pro}$ inhibitors obtained from high-throughput screening.

4.2 From Rational Drug Design

4.2.1 Peptidomimetics

4.2.1.1 AG7088 Analogues

Dragovich et al. synthesized a series of compounds targeting rhinovirus 3C protease for the possible treatment of the human common cold [39]. The best inhibitor is AG7088, a ketomethyl isostere of a tripeptide-conjugated ester (a peptide-like rhinovirus 3C protease inhibitor) with an EC_{50} value of 0.013 μM in inhibiting the rhinovirus protease [40, 41]. Its P1 is a γ-lactam moiety to mimic the P1 glutamine residue, and P1′ is an α,β-unsaturated ester that acts as a Michael acceptor to inhibit the rhinovirus $3C^{pro}$ by forming a covalent bond with the active site Cys residue. To improve cell membrane permeability, the P2 phenylalanine residue was replaced with a methylene isostere bearing a 4-fluorophenyl substituent. Although it was a potent inhibitor of the rhinovirus $3C^{pro}$, it was not approved for clinical use due to a lack of obvious advantage in treating patients with common cold. He et al. from Agouron Pharmaceuticals, Inc., applied for a US patent entitled "Inhibitors of SARS 3C like protease" for the application of the AG7088-like compounds with Michael acceptor to inhibit the SARS-CoV $3CL^{pro}$. Two formulae were proposed as potential SARS protease inhibitors (**13** and **14**, Fig. 5) without giving their activity data [42]. Kania et al. from Pfizer, Inc., developed a series of compounds with the same structural features of γ-lactam at P1 and a isobutyl group at P2 to inhibit SARS-CoV $3CL^{pro}$, as described in their world patent entitled "Anticoronaviral compounds and compositions, their pharmaceutical uses and materials for their synthesis" [43]. These compounds were shown to provide protection for the Vero cells from HCoV 229E and SARS-CoV infection in a viability assay. Although having the same structural features, some of these compounds were inactive (EC_{50} > 100 μM) against the SARS-CoV and some showed inhibitory activity. The best compound of this series displayed

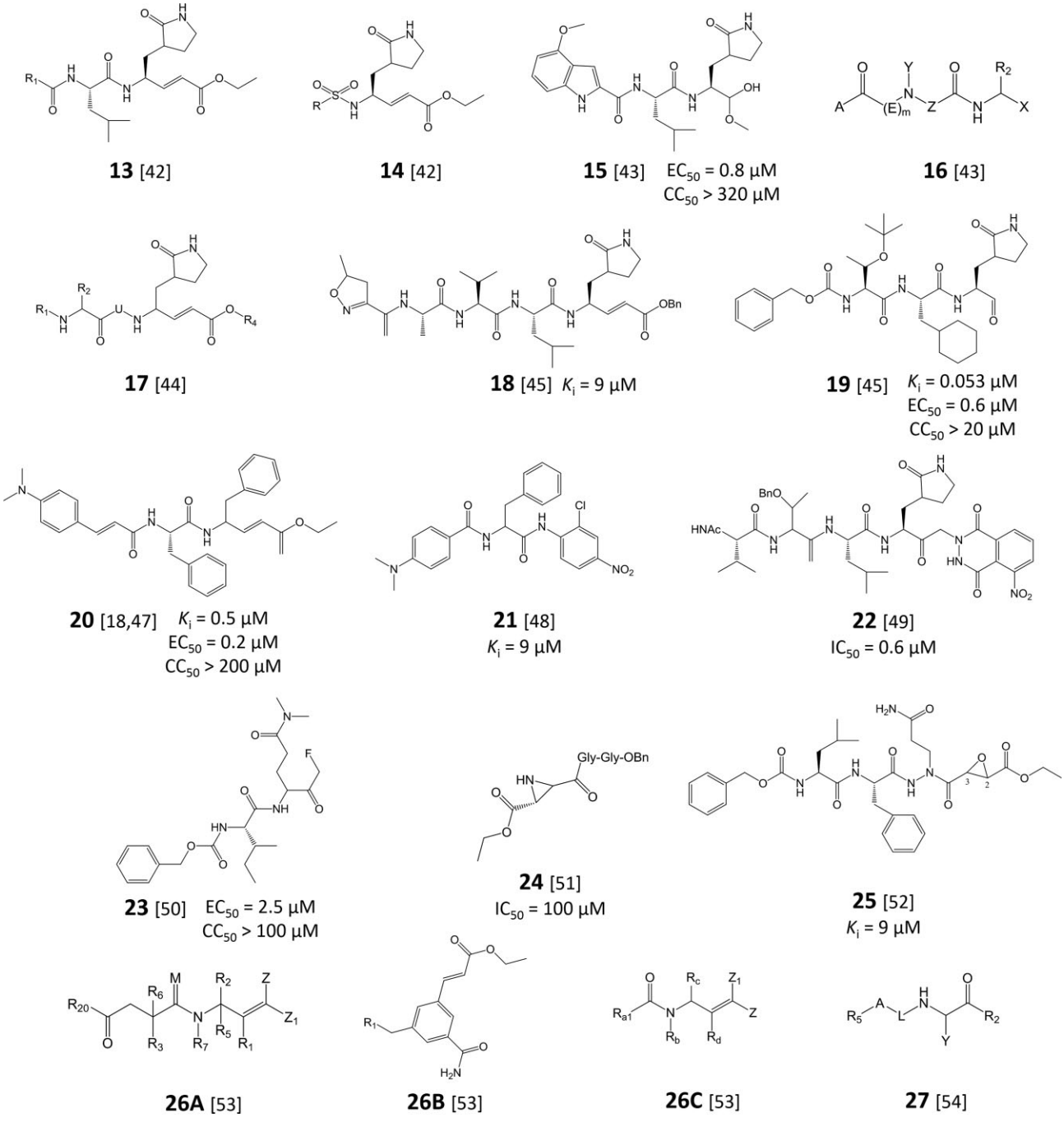

Figure 5. Peptidomimetics as SARS-CoV $3CL^{pro}$ inhibitors.

an EC_{50} value of 0.8 μM (**15**, Fig. 5) to inhibit SARS-CoV replication by targeting the SARS-CoV $3CL^{pro}$ without toxicity (CC_{50} > 320 μM). A general formula is given in Fig. 5 (**16**). Rao et al. applied for a patent covering a series of AG7088 analogues with the common structure of compound **17** (Fig. 5) as inhibitors of SARS $3CL^{pro}$ [44]. Using a continuous fluorometric assay with the fluorogenic substrate MCA-AVLQSGFR-Lys(Dnp)Lys-NH_2, an effective compound (**18**, Fig. 5) in this series inhibited not only the $3CL^{pro}$ of SARS-CoV (K_i = 9 μM, k_{inact} (rate of enzyme inactivation) = 0.0031 s^{-1}), but also the protease of HCoV 229E, TGEV, feline infectious peritonitis virus, mouse hepatitis virus, and infectious bronchitis virus [45]. This compound exhibited an EC_{50} value of 4.3 μM against mouse hepatitis virus on murine delay brain tumour cells in a plaque-reduction assay. It also has low toxicity (500 μM compound only displayed 28 % inhibition of cell growth). Yang et al. discovered a potent inhibitor from the AG7088 analogues with cyclic γ-lactam at the P1 position, TG-0205221 (K_i =

0.053 μM for compound **19**, Fig. 5), based on the HPLC assay [45]. The inhibitor exhibited potent activities in suppressing replication of SARS-CoV (4.7 log viral titer reduction at 5 μM concentration, EC_{50} = 0.6 μM and cytotoxicity CC_{50} > 20 μM) and HCoV 229E (5.2 log viral titer reduction at 1.25 μM concentration, EC_{50} = 0.14 μM). The tight binding between TG-0205221 and the SARS-CoV $3CL^{pro}$ is through a covalent bond, hydrogen bonds, and unprecedented hydrophobic interactions as evidenced by the crystal structure of the corresponding complex [46]. Shie et al. found that the replacement of the γ-lactam moiety in AG7088 with a phenylalanine side chain resulted in a more potent SARS-CoV $3CL^{pro}$ inhibitor [47]. As shown in Fig. 5, the best inhibitor (**20**) of this series has a K_i value of 0.5 μM measured by the Edans-Dabcyl FRET assay. The compound also showed potent activity (EC_{50} = 0.2 μM) against SARS-CoV replication by blocking the synthesis of the viral spike protein without apparent toxicity (CC_{50} > 200 μM) in cell-based assays [47]. From the computer modelling, the phenylalanine side chain at P1 and P2 positions may be shifted by one position to occupy S2 and S3 sites as the α,β-unsaturated Michael acceptor is not covalently bound with the Cys145. According to the product-bound crystal structure of the SARS-CoV $3CL^{pro}$ [18], S2 is a hydrophobic pocket to hold the hydrophobic residue, and the P3 side chain is exposed to the solvent.

4.2.1.2 Anilides

A series of peptide anilides with aniline derivatives, such as 2-chloro-4-nitroaniline, next to L-phenylalanine were shown to inhibit the SARS-CoV $3CL^{pro}$ and also the viral replication [48]. Compound **21** shown in Fig. 5 is the most potent inhibitor of SARS-CoV $3CL^{pro}$ with a K_i value of 0.03 μM using the Edans-Dabcyl FRET assay. Deletion of the chloro, nitro, or dimethylamino substituents from this compound significantly weakened the binding affinity. Also, replacing the dimethylamino group with a nitro group caused a reduction in inhibitor potency. According to the molecular docking, the nitro group of the compound is predicted to be hydrogen bonded with the NH of Ala46, while the chlorine atom is within 3 Å from the γ-S atom of Cys145 and the Nε2 atom of His41, therefore providing a possible key interaction with the catalytic dyad.

4.2.1.3 Keto-Glutamine Analogues

As the SARS-CoV $3CL^{pro}$ recognizes a glutamine residue at the P1 site, Jain et al. synthesized and evaluated a series of keto-glutamine analogues with a phthalhydrazido group at the α position as reversible protease inhibitors [49]. Attachment of a tripeptide (Ac-Val-Thr-Leu) to these glutamine-based "warheads" resulted in significantly better inhibitors. N,N-dimethyl-glutamine analogues are much less potent inhibitors (10- to 100-fold larger IC_{50}) than cyclic glutamine analogues. The best inhibitor (**22**, Fig. 5) showed an IC_{50} value of 0.6 μM measured using an Abz-Tyr(NO_2) FRET assay. In the modelling structures, the inhibitor is bound in an extended conformation, forming a partial β-sheet and a hydrogen bond between His163 and the P1 side chain. The modelling studies indicate that the active site of the enzyme has enough room to accommodate the bulky phthalhydrazido group. Some rearrangements of the protein, in particular residue Glu166, are required to accommodate the extra bulky group on the P1 residues.

4.2.1.4 Glutaminyl Fluoromethyl Ketones

Zhang et al. have designed and synthesized a series of dipeptidyl glutaminyl fluoromethyl ketones (**23**, Fig. 5) to covalently inhibit the SARS-CoV $3CL^{pro}$ by reacting with the active site Cys residue [50]. These inhibitors were synthesized by using N,N-dimethyl-Gln-fmk as the P1 residue and warhead, in combination with different P2 amino acids via five-step reactions. The dipeptides with hydrophobic residues such as Leu, Val, and Phe at P2 position showed a better effect against SARS-CoV infected Vero cells, consistent with the protease substrate preference. The best inhibitor, as shown in Fig. 5, has an EC_{50} value of 2.5 μM tested with the Vero cells. The toxicity CC_{50} value of the inhibitor is > 100 μM. However, the compounds with Gly and Ala as the P2 amino acid did not inhibit the viral replication.

4.2.1.5 Aziridinyl Peptide

Similar to fluoromethyl ketones, aziridine and epoxide can also react with nucleophilic amino acids within the active site of proteases. The screening using HPLC-based and FRET-based assays have identified a *trans*-configuration N-substituted aziridine-2,3-dicarboxylate, named (S,S) (C_2H_5O) Azi-Gly-Gly-OBn (**24**, Fig. 5), as a modest inhibitor of SARS-CoV $3CL^{pro}$ (54% enzyme activity was inhibited by 100 μM compound) [51]. This activity may be enhanced by linking the electrophilic building blocks to appropriate amino acids (e.g., Gln), substrate analogous peptides, or peptidomimetics.

4.2.1.6 Aza-peptide Epoxide

An aza-peptide epoxide (**25**, Fig. 5) was also found to inhibit SARS-CoV $3CL^{pro}$ covalently with a K_i value of 18 μM and k_{inact} of 35×10^{-3} s^{-1} [52]. According to the complex crystal structure, the epoxide ring of the inhibitor opens upon Cys attacking, leaving a hydroxyl group on the C2 atom to form hydrogen bonds with the Asn142 Oδ1 atom of the protease (2.9 Å) and the P2-Phe carbonyl O atom of the inhibitor (3.2 Å). The configurations of the C2 and C3 atoms are inverted from S,S to R,R.

4.2.1.7 Miscellaneous

Shella et al. applied for a patent entitled "Inhibitors of severe acute respiratory syndrome (SARS) SARS-CoV $3CL^{pro}$" [53]. They discovered pharmaceutical peptide-like compounds, including three components (**26A**, **26B**, and **26C**, Fig. 5), which inhibited SARS and rhinovirus $3C^{pro}$ in a mammal by administering effective amounts of the rhinovirus $3C^{pro}$ inhibitors. However, no assay data are available. Cai et al. found that the compounds with the general structure of compound **27** (Fig. 5) can inhibit SARS-CoV $3CL^{pro}$ in SARS-CoV and feline infectious peritonitis virus, as described in their patent entitled "Protease inhibitors for coronaviruses and SARS-CoV and the use thereof" [54]. The inventors performed cell-based assays using infected cells, such as the murine delay brain tumor cells infected by mouse hepatitis virus strain A59 or the Vero cells

infected by SARS-CoV, and found that these compounds could inhibit the viruses and protect the cells from infection. They further suggest the compounds may be administered to mammals, such as humans, orally at a dose of 0.0025–50 mg kg^{-1}, or an equivalent amount of the pharmaceutically acceptable salt thereof, per day of the body weight when the mammals are being treated for SARS-CoV or other CoV-mediated disorders. Preferably, ~0.001–10 mg kg^{-1} is orally administered to treat or prevent such disorders. For intramuscular injection, the dose is generally ~50 % of the oral dose.

4.2.2 Non-Peptidomimetic Inhibitors

4.2.2.1 Isatin

Certain isatin (2,3-dioxindole) derivatives are known potent inhibitors against the rhinovirus $3C^{pro}$ [55]. This isatin core structure offers several advantages that include ease of synthesis and chemical modification. Its derivatives were tested as inhibitors for SARS $3CL^{pro}$. A series of synthetic isatin derivatives showed IC_{50} values in the range of 0.95–17.5 μM from an Edans-Dabcyl FRET assay and confirmed by a HPLC-based assay, and the best inhibitor found is listed in Fig. 6 (**28**), which has an iodine or brom atom in the isatin scaffold [56]. It can be concluded that the benzothiophenemethyl side chain provides more inhibitory effect than the benzyl, heterocyclic substituted methyl, and other alkyl groups. Recently, Zhou et al. have reported a series of N-substituted isatin derivatives against SARS-CoV $3CL^{pro}$ [57]. The inhibition activity was measured by the continuous colorimetric assay using the colorimetric substrate Thr-Ser-Ala-Val-Leu-Gln-pNA. The C-5 position of isatin was found to favor a carboxamide group and the N-1 position to favor large hydrophobic substituents for inhibiting the protease. The lowest IC_{50} value (0.37 μM) was observed among these inhibitors.

4.2.2.2 Metal-Conjugated Inhibitors

As shown above in high-throughput screening of 960 compounds, 2 compounds (phenylmercuric acetate and thimerosal) identified as potent SARS-CoV $3CL^{pro}$ inhibitors contain mercury (**9** and **10**, Fig. 4). This suggests the use of a metal ion as a chelator for Cys proteases as metal ions such as Hg^{2+}, Zn^{2+}, and Cu^{2+} have high affinities to the sulfur atom of the Cys residue [58, 59]. As mercury-containing compounds may pose therapeutic hazards to a patient if orally taken, a series of zinc-containing compounds and metal ions were evaluated for SARS-CoV $3CL^{pro}$ inhibition [33]. The most potent inhibitor found was 1-hydroxypyridine-2-thione zinc, a competitive inhibitor with a K_i value of 0.17 μM (**29**, Fig. 6) with more inhibitory activity than just Zn^{2+} (K_i = 1.1 μM). Zn^{2+} was previously found to be tetrahedrally coordinated by three Cys sulfurs and one His nitrogen of the 2A protease from a common cold virus, which is responsible for the shut-off of host-cell protein synthesis [60]. Zinc-containing compounds, such as zinc acetate, are added as a supplement to the drug for the treatment of Wilson's disease [61], indicating the safety of the ion for human use. Zinc salts such as zincum gluconicum (Zenullose) may be effective in treating the common cold, a disease caused by rhinoviruses, without knowledge of the molecular target [62]. Moreover, zinc ions inhibit the replication of rhinoviruses [63, 64]. Thus, the potential use of the zinc-conjugated compounds as a therapeutic treatment of the SARS disease needs to be explored.

4.2.2.3 Aryl Boronic Compounds

Bacha et al. proposed an attractive subsite for the design of potent inhibitors (**30**, Fig. 6), which is a cluster of Ser residues (Ser139, Ser144, and Ser147) close to the catalytic residues [65]. In fact, this Ser cluster is conserved in all known CoV proteases and may represent a common target of wide-spectrum CoV protease inhibitors. Based on the known reactivity of boronic acid compounds with the hydroxyl group in Ser residues, the inhibitory potency of bifunctional boronic acid compounds was evaluated. A chemical scaffold containing two phenyl boronic groups attached to a central aromatic ring by ester linkages were tested. This compound has a K_i value of 0.04 μM based on an Edans-Dabcyl FRET assay. Different variations of the compound were prepared, including several isomers with replacement of the central aromatic ring with shorter ester linkage and different functionalities at the phenyl boronic rings. The highest improvement in affinity was observed when the ester linkage between the aromatic rings was replaced with an amide group, thereby resulting in nanomolar inhibition constants. The inhibitors display a mixed competitive pattern and bind to both free enzyme and enzyme substrate complex. This may be due to the large substrate used in the kinetic measurements. These compounds inhibited the enzyme in a reversible manner. Freire et al. provided a series of organic boron-containing compounds (compound **31** as a representative and **31A**, **31B**, and **31C** as examples in Fig. 6), compositions thereof and methods of using such compounds and compositions for inhibiting CoV proteases and for treating infections [66]. The invention provides a method of inhibiting CoV proteases, treating infections caused by CoV and detecting CoV, particularly CoV proteases that have one or more serine or threonine residue(s) at or near its active site and proteases of SARS-associated CoV. Such methods comprise contacting the testing sample obtained from a patient with boron-containing compound **31** [66] that have been: i) tethered to an appropriate surface such that protease coming into contact and being bound to the tethered compound can be detected; ii) labelled by fluorescent, radioactive, or other markers that allow identification of CoV protease bound to the compound; or iii) that by any other means can be used to detect the presence of CoV protease.

4.2.2.4 Etacrynic Acid

As shown above, fluoromethyl ketones and aziridinyl peptides are active-site-directed inhibitors. These scrutinized compounds contain electrophilic building blocks (aziridine, epoxide, Michael system) that are known to react with nucleophilic amino acids within the active site of proteases. Derivatives of etacrynic acid, a well-known diuretic drug containing an activated double bond, were also shown as non-peptidic SARS-CoV $3CL^{pro}$ inhibitors. A comprehensive screening with an HPLC-based assay was performed for SARS-CoV $3CL^{pro}$. The

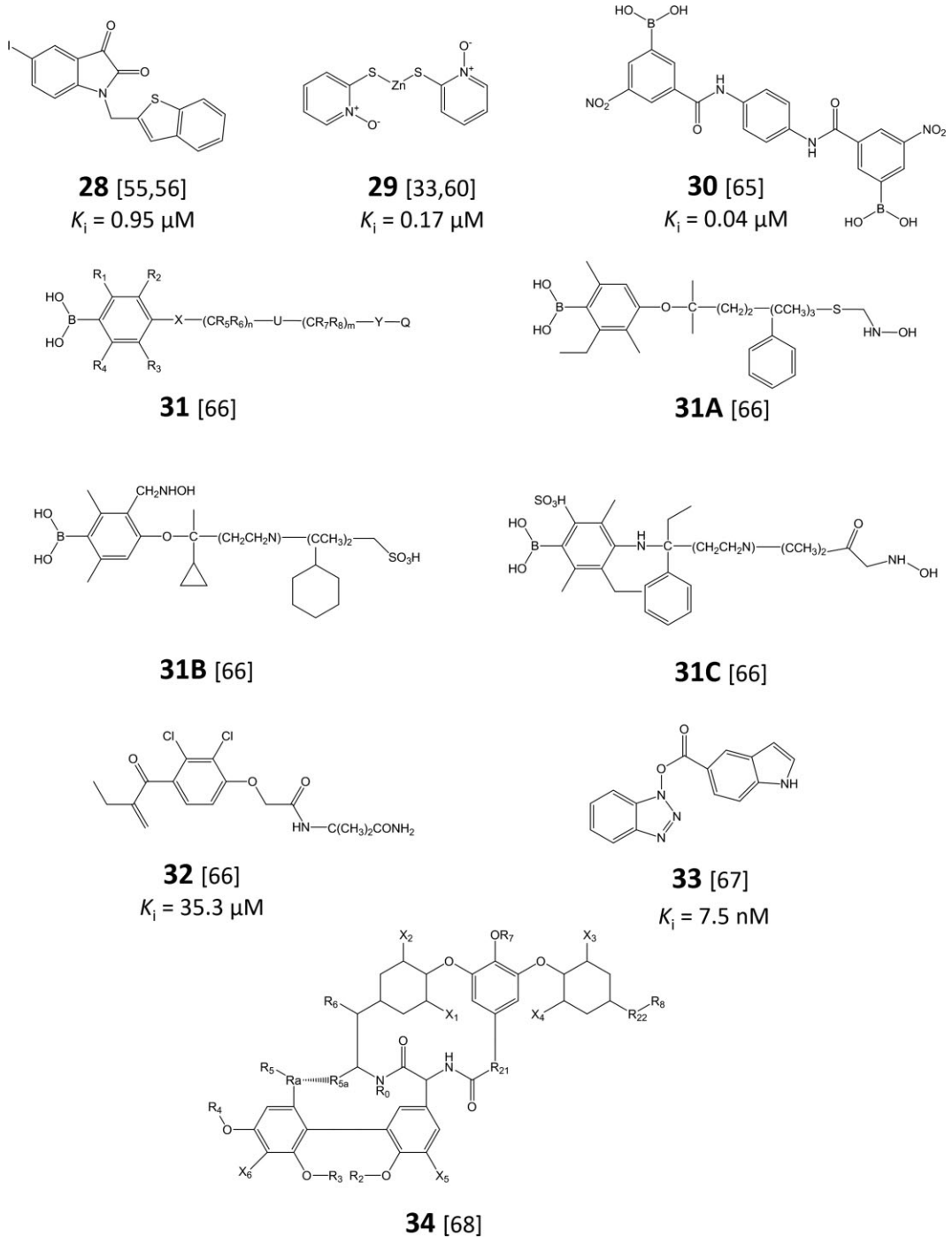

Figure 6. Non-peptidomimetic inhibitors of SARS-CoV 3CL^{pro}.

most promising inhibitor, etacrynic acid tert-butylamide (**32**, Fig. 6) inhibits the protease (K_i = 35.3 μM, measured through a FRET assay).

4.2.2.5 Benzotriazoles

A class of stable benzotriazole esters were reported as mechanism-based inactivators of the SARS-CoV 3CL^{pro} [67]. During the preparation of a library of lopinavir-like compounds, various carboxylic acids were coupled with the amines in the presence of 2-(1H-benzotriazole-1-yl)-1,1,3,3-tetramethyluronium hexafluorophosphate (HBTU) and the intermediates of the acids with HBTU were found to inhibit the protease. The compounds were purified and characterized and the most potent inhibitor (**33**, Figure 6) showed a K_i value of 7.5 nM. It is a covalent inhibitor and specifically acylates the Cys145 residue with a k_{inact} of 0.0011 s^{-1}.

4.2.2.6 Glycopeptides

Balzarini et al. patented novel glycopeptide antibiotic derivatives, such as compound **34** (Fig. 6), for the processes of their preparation, their use as a medicine, their use in treating or preventing viral infections and their use in manufacturing a medicine to treat or prevent viral infections [68]. The invention covers the use of glycopeptide antibiotics including vancomycin, teicoplanin, ristomycin, eremimycin-type aglycons, and their semisynthetic derivatives to treat or prevent viral infections, especially the infections by the viruses belonging to Retroviridae, Herpesviridae, Flaviviridae, and Coronaviridae, such as HIV, hepatitis C virus, bovine viral diarrhoea virus, SARS-CoV, feline CoV, herpes simplex virus, varicella zoster virus, and cytomegalovirus.

4.3 By Computer Modelling

4.3.1 Phenylsulfonyl Pyridine

Lu et al. performed a structure-based virtual screening of a chemical database containing 58855 compounds followed by testing the potential inhibitors against SARS-CoV $3CL^{pro}$ to identify 2 hits [69]. One of the hits was a 6-methoxy-3-nitro-2-(phenylsulfonyl) pyridine with an IC_{50} value of 0.3 μM (**35**, Fig. 7) measured using Edans-Dabcyl FRET assay. The core structure (diphenyl sulfone) of this compound was used to search for other analogues and the analogues were measured for their inhibition constants against SARS protease. Wu et al. have filed a patent that relates to a method for modulating activity of SARS-CoV $3CL^{pro}$ or an analogue thereof by contacting the protein with an effective amount of the series of diphenyl sulfone analogues [70]. This invention is based on the discovery that a group of dicyclic or multi-cyclic compounds effectively inhibit the activity of SARS-CoV $3CL^{pro}$ and hepatitis C virus NS3 protease, a structural analogue of SARS-CoV $3CL^{pro}$.

4.3.2 Oxadiazol-imidazole

Another compound identified in virtual screening by Lu et al. was 2-({[3-(4-chlorophenyl)-1,2,4-oxadiazol-5-yl]methyl}thio)-4,5-dihydro-1H-imidazol-3-ium chloride with an IC_{50} value of 3 μM against SARS-CoV $3CL^{pro}$ (**36**, Fig. 7) [69]. The core structure as shown in bold was used to search for the structural analogues; nine compounds with moderate structural similarity were found to inhibit the SARS-CoV $3CL^{pro}$ [69].

4.3.3 N-phenyl-2-(pyrimidinylthio)acetamide

Using virtual screening and 3D-QSAR studies, Tsai et al. discovered a group of SARS-CoV $3CL^{pro}$ inhibitors called Nphenyl-2-(pyrimidinylthio) acetamide [71] and filed a patent application [72]. The most potent one (**37**) of these analogues, with an IC_{50} value of 3 μM from an Edans-Dabcyl FRET assay, is shown in Fig. 7. The core structure is highlighted in bold.

4.3.4 Cinanserin

Chen et al. performed virtual screening on the existing medical database CMC (Comprehensive Medicinal Chemistry, MDL Information System, Inc.) for SARS-CoV $3CL^{pro}$ inhibitors by using its three-dimensional structure. Cinanserin (**38**, Fig. 7) was identified to inhibit the protease [73] and two patents were filed [74, 75]. The IC_{50} values of cinanserin for inhibiting SARS-CoV $3CL^{pro}$ and HCoV 3CL protease were found to be 4.9 and 4.7 μM, respectively, using an Edans-Dabcyl FRET assay. Cinanserin was also found to block SARS-CoV replication

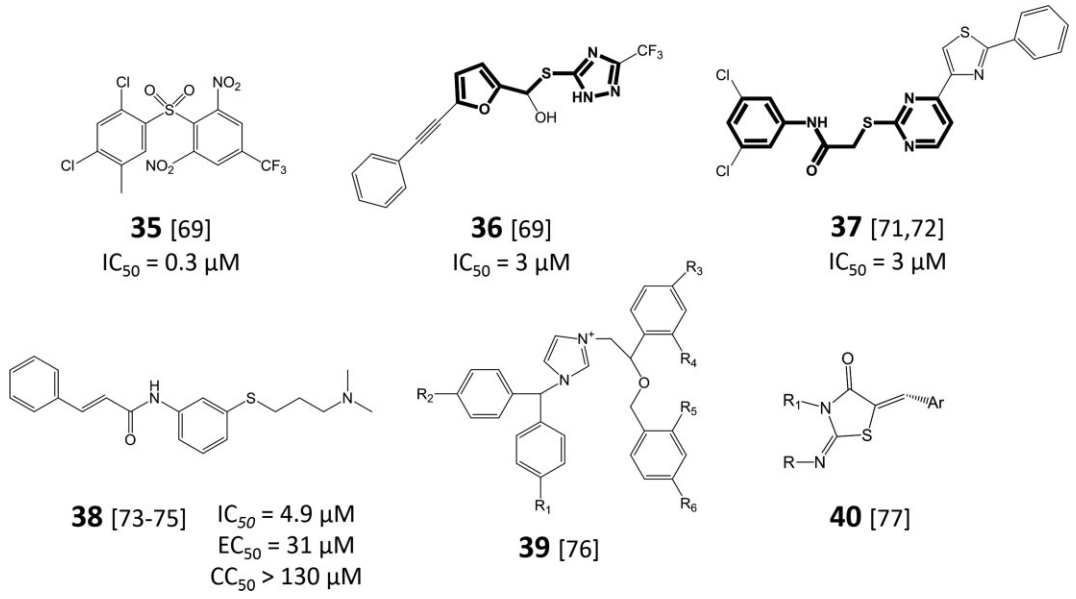

Figure 7. Inhibitors of SARS-CoV $3CL^{pro}$ derived from computer modeling.

in tissue culture. Treatment of the cells with 50 μg-ml^{-1} (134 μM) cinanserin reduced the SARS-CoV RNA concentration by > 3 log units with an EC_{50} value of 31 μM. The reduction of the titre of infectious particles exactly corresponded to the reduction in virus RNA concentration. No toxicity of the compound was detected in the concentration range tested (≤ 130 μM).

4.3.5 Calamidazolium Compound

Lai et al. used computer modelling to simulate a three-dimensional structure of SARS-CoV 3CL^{pro} and obtained calamidazolium (**39**, Fig. 7) as a potential inhibitor [76]. HPLC assays were further used to verify that the compound indeed inhibits the enzyme.

4.3.6 5-Benzylidene-4-oxo-1,3-thiazolidin Analogues

Shen et al. used the structure (PDB ID 1LVO) of TGEV M^{pro} as the template to simulate the structural model of SARS-CoV 3CL^{pro} and identified the active site. Through molecular docking, they screened compounds from a commercial data bank for active-site inhibitors. A series of 5-benzylidene-4-oxo-1,3-thiazolidin analogues with the core structure as compound **40** (Fig. 7) were found to inhibit the recombinant SARS 3CL^{pro} and prevent the virus infection on Vero-E6 cells [77].

5 Engineering of SARS-CoV 3CL^{pro}

In addition to serving as a promising target in anti-SARS chemotherapy, SARS-CoV 3CL^{pro} possesses potential as a tag-cleavage endopeptidase. As analogous to picornaviruses 3C proteases, 3CL^{pro} has substrate specificity in cleaving the amide bond between P1-Gln and a small amino acid such as Ser, Ala, or Gly at P1′ [78, 79]. According to the structure of SARS-CoV 3CL^{pro} [10, 18], this small P1′ residue is near Thr25, which likely limits the substrate specificity. Since the recombinant SARS-CoV 3CL^{pro} can undergo auto-processing [18, 80], a modification on the S1′ might tolerate a large amino acid at P1′ position. In fact, SARS-CoV 3CL^{pro} with T25G mutation expands the S1′ site and, thus, is able to cleave peptides with larger amino acids such as Met (the starting amino acid of most native proteins) at P1′ [81] (Fig. 8a). Indeed, compared with the k_{cat} of 1.6 ± 0.2 min^{-1} and the K_m of 76.6 ± 3.5 μM for the wild-type, the T25G mutant displays the k_{cat} of 16.2 ± 0.5 min^{-1} and the K_m of 18.6 ± 2.4 μM (43.5-fold higher k_{cat}/K_m) against the SAVLQ↓MGFRK substrate. Moreover, vectors that contain the nucleotides encoding the T25G recognition site AVLQ↓M between the tags and the N-terminal Met of the target proteins have been constructed and expressed by the prokaryotic and eukaryotic hosts. In these vectors, *Pst*I (CTGCAG) is chosen as a 5′ cloning site, since its sequence overlaps with the nucleotide sequence (GCGGTGCTGCAG) encoding the protease recognition site (Fig. 8B). Identical 5′-*Pst*I/3′-*Xho*I cloning sites in these vectors can be used to allow sticky-end DNA fragments of the target genes generated by PCR [82] to ligate with these

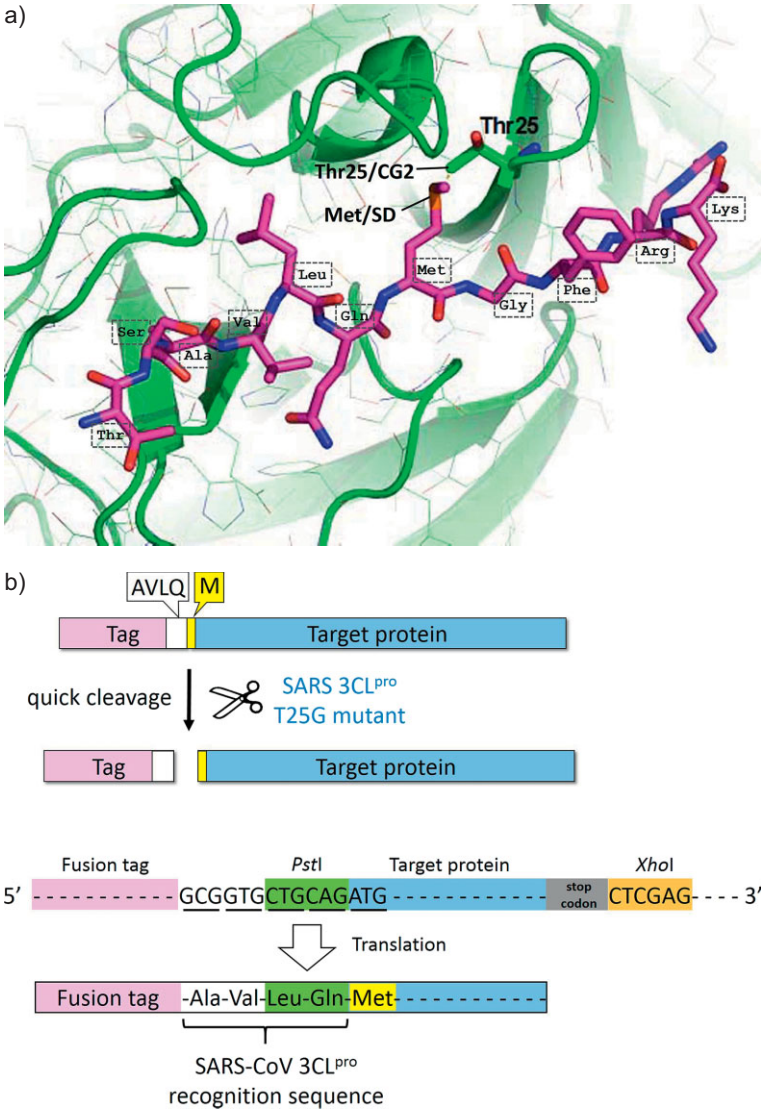

Figure 8. Engineering of SARS-CoV 3CL^{pro} as an endopeptidase. (a) Structural basis for Thr25 mutation. Predicted structural model of SARS-CoV 3CL^{pro} with a modified peptide containing Met at P1′ (Thr-Ser-Ala-Val-Leu-Gln-Met-Gly-Phe-Arg-Lys, as indicated), based on the crystal structure of the SARS-CoV 3CL^{pro} H41A mutant in complex with a peptide (PDB ID 2Q6G). (b) Schematic illustration of the expression of a target protein with a tag and the engineered cleavage site. The fusion protein can be cleaved by T25G mutant SARS-CoV 3CL^{pro} between AVLQ and Met at P1′ (upper panel); strategy of using *Pst*I as a 5′ cloning site (CTGCAG) that is part of the sequence GCGGTGCTGCAG encoding the protease recognition sequence AVLQ (lower panel).

vectors simultaneously (parallel cloning method) [83, 84]. These engineered vectors and the T25G mutant can be assembled as a kit for the maximal production of soluble and functional proteins with authentic sequences (see the patent entitled "Protein expression system involving mutated severe respiratory syndrome-associated coronavirus 3C-like protease" by Liang et al. [85]).

6 Conclusions

Since viral protease inhibitors are remarkably effective at blocking the viral replication and virus-induced cytopathic effects, inhibiting $3CL^{pro}$ proteolysis is a convincing strategy against SARS-CoV. In this review article, the effective inhibitors against SARS-CoV $3CL^{pro}$ are summarized and the methodology for detecting the protease activity and inhibitor screening are discussed. Most of the peptidomimetic inhibitors of the SARS-CoV $3CL^{pro}$ are designed based on its substrate specificity of P1-Gln, but some have Phe to replace the Gln moiety. For covalent inhibitors, the electrophilic structural features, such as Michael acceptor (α,β-unsaturated ester), fluoromethyl ketone, aziridine, epoxide, and etacrynic acid, are built in to react with the active-site Cys residue. The metal-containing compounds also target the Cys145 residue. Other compounds that have been suggested to bind to the active site of SARS protease based on computer modelling are potential inhibitors. All the inhibitors for SARS-CoV $3CL^{pro}$ may also be used in inhibiting other viral proteases due to some degree of structural similarity of their active sites. In fact, some of the SARS-CoV $3CL^{pro}$ inhibitors are derived from previously identified rhinovirus $3C^{pro}$ inhibitors such as AG7088 (now called Rupintrivir). Rupintrivir is a potent inhibitor of $3C^{pro}$ based on in vitro and in vivo studies. Its analogues modified based on the structural differences between $3C^{pro}$ and $3CL^{pro}$ represent promising leads for anti-CoV agents.

Several classes of $3CL^{pro}$ inhibitors can also inhibit picornaviral $3C^{pro}$ [86]. Structural studies have revealed that $3C^{pro}$ is a monomer, whereas $3CL^{pro}$ is a dimeric protein which has an extra third domain for dimer formation, although their active sites are superimposed very well [87]. Moreover, $3C^{pro}$ has a more open but shallow S2 site, as well as a smaller S3 site, which account for different inhibitory specificity, as concluded from the structural comparison of the same inhibitor in the $3C^{pro}$ and $3CL^{pro}$ active sites [86]. Moreover, these inhibitors could possibly serve as new drug leads for other viral diseases such as those caused by rhinovirus, HCoV 229E, enterovirus, transmissible gastroenteritis virus, feline infectious peritonitis virus, mouse hepatitis virus, and infectious bronchitis virus. Particularly, the recently emerged SARS-like coronavirus, human betacoronavirus 2c EMC/2012 (HCoV-EMC), also called Middle East respiratory syndrome coronavirus (MERS-CoV), has a $3CL^{pro}$ structurally similar to SARS-CoV $3CL^{pro}$ and the protease can be inhibited by N3 (**18**, Fig. 5) [88], which is a Rupintrivir analogue inhibiting SARS-CoV $3CL^{pro}$. Moreover, CE-5, a small-molecule inhibitor of $3CL^{pro}$ of SARS-CoV [89] also inhibits the activity of MERS-CoV $3CL^{pro}$ [90]. Therefore, the information discussed in the present review helps to ultimately develop drugs against infectious CoVs and picornaviruses, which should be continuously pursued.

A mutant (T25G) of SARS $3CL^{pro}$ can recognize Ala-Val-Leu-Gln↓Met and cleave the fusion proteins efficiently. As a result, it can serve as a novel endopeptidase for tag cleavage when the fusion proteins expressed in *E. coli* and yeast *Pichia* contain the AVLQ sequence immediately before their own N-terminal Met residue. Moreover, the mutant protease also showed similar cleavage efficiency to the commonly used FXa in cleaving the tag under the same condition. Other vectors with different expression systems including baculovirus-infected insect cells, mammalian cells, and cell-free system, could also be constructed to contain the same protease recognition site. The common 5′-*Pst*I/3′-*Xho*I restriction sites can be used for parallel cloning of the sticky-end PCR product of a target gene into these vectors. These engineered vectors and the mutant protease can be assembled as a kit for parallel expression of a target gene in multiple hosts simultaneously to screen for the most optimal condition to produce a soluble and functional protein with maximal yield. The fusion protein can then be purified with the affinity column against the tag (e.g., NiNTA for His-tag) and the tag can be removed by T25G $3CL^{pro}$ to yield the recombinant protein with authentic sequence.

The authors have declared no conflict of interest.

Chih-Jung Kuo received his doctorate from National Taiwan University in 2009 under the supervision of Dr. Po-Huang Liang. In his dissertation he developed a fluorogenic substrate for the activity detection of SARS 3C-like protease and inhibitor screening. He then worked as a Postdoctoral Fellow in Chang's group at Cornell University, Department of Population Medicine and Diagnostic Sciences from 2009–2013. Currently, he is an assistant professor in the Department of Veterinary Medicine at National Chung Hsing University in Taiwan.

Po-Huang Liang currently is a Research Fellow in the Institute of Biological Chemistry, Academia Sinica, and a Joint Professor in the Institute of Biochemical Sciences, National Taiwan University, Taiwan. His research theme is enzymology and mechanism-based drug discovery and enzyme engineering, with working subjects of enzymology of prenyltransferases, mechanistic approaches to discover anti-viral and anti-cancer drugs and mechanism-based enzyme engineering for biofuel production.

Symbols used

K_D	[M]	dimer dissociation constant
K_i	[M]	inhibition constant
k_{inact}	[s^{-1}]	rate of enzyme inactivation

Abbreviations

$3CL^{pro}$	3C-like protease
$3C^{pro}$	3C protease
AUC	analytic ultracentrifugation
CC_{50}	half maximal cytostatic concentration
CMC	Comprehensive Medicinal Chemistry
CoV	coronavirus
E	envelope
EC_{50}	half maximal effective concentration
FRET	fluorescence resonance energy transfer
HBTU	2-(1H-benzotriazole-1-yl)-1,1,3,3-tetramethyl-uronium hexafluorophosphate
HCoV	human coronavirus
IC_{50}	half maximal inhibitory concentration
M	membrane glycoproteins
M^{pro}	main protease
N	nucleocapsid protein
nsp	nonstructural protein
ORF	open reading frames
RP-HPLC	reverse-phase high-pressure liquid chromatography
S	spike
SARS	severe acute respiratory syndrome
TF2B	3-isotheaflavin-3-gallate
TFA	trifluoroacetic acid
TGEV	transmissible gastroenteritis virus

References

[1] A. S. Monto, *Rev. Infect. Dis.* **1989**, *11 (3)*, 498–505. DOI: 10.1093/clinids/11.3.498

[2] C. Drosten, S. Gunther, W. Preiser, S. van der Werf, H. R. Brodt, S. Becker, H. Rabenau, M. Panning, L. Kolesnikova, R. A. Fouchier, A. Berger, A. M. Burguiere, J. Cinatl, M. Eickmann, N. Escriou, K. Grywna, S. Kramme, J. C. Manuguerra, S. Muller, V. Rickerts, M. Sturmer, S. Vieth, H. D. Klenk, A. D. Osterhaus, H. Schmitz, H. W. Doerr, *N. Engl. J. Med.* **2003**, *348 (20)*, 1967–1976. DOI: 10.1056/NEJMoa030747

[3] T. G. Ksiazek, D. Erdman, C. S. Goldsmith, S. R. Zaki, T. Peret, S. Emery, S. Tong, C. Urbani, J. A. Comer, W. Lim, P. E. Rollin, S. F. Dowell, A. E. Ling, C. D. Humphrey, W. J. Shieh, J. Guarner, C. D. Paddock, P. Rota, B. Fields, J. DeRisi, J. Y. Yang, N. Cox, J. M. Hughes, J. W. LeDuc, W. J. Bellini, L. J. Anderson, S. W. Group, *N. Engl. J. Med.* **2003**, *348 (20)*, 1953–1966. DOI: 10.1056/NEJMoa030781

[4] J. S. Peiris, S. T. Lai, L. L. Poon, Y. Guan, L. Y. Yam, W. Lim, J. Nicholls, W. K. Yee, W. W. Yan, M. T. Cheung, V. C. Cheng, K. H. Chan, D. N. Tsang, R. W. Yung, T. K. Ng, K. Y. Yuen, *Lancet* **2003**, *361 (9366)*, 1319–1325. DOI: 10.1016/S0140-6736(03)13077-2

[5] P. A. Rota, M. S. Oberste, S. S. Monroe, W. A. Nix, R. Campagnoli, J. P. Icenogle, S. Penaranda, B. Bankamp, K. Maher, M. H. Chen, S. Tong, A. Tamin, L. Lowe, M. Frace, J. L. DeRisi, Q. Chen, D. Wang, D. D. Erdman, T. C. Peret, C. Burns, T. G. Ksiazek, P. E. Rollin, A. Sanchez, S. Liffick, B. Holloway, J. Limor, K. McCaustland, M. Olsen-Rasmussen, R. Fouchier, S. Gunther, A. D. Osterhaus, C. Drosten, M. A. Pallansch, L. J. Anderson, W. J. Bellini, *Science* **2003**, *300 (5624)*, 1394–1399. DOI: 10.1126/science.1085952

[6] S. M. E. C. Chinese, *Science* **2004**, *303 (5664)*, 1666–1669. DOI: 10.1126/science.1092002

[7] M. A. Marra, S. J. Jones, C. R. Astell, R. A. Holt, A. Brooks-Wilson, Y. S. Butterfield, J. Khattra, J. K. Asano, S. A. Barber, S. Y. Chan, A. Cloutier, S. M. Coughlin, D. Freeman, N. Girn, O. L. Griffith, S. R. Leach, M. Mayo, H. McDonald, S. B. Montgomery, P. K. Pandoh, A. S. Petrescu, A. G. Robertson, J. E. Schein, A. Siddiqui, D. E. Smailus, J. M. Stott, G. S. Yang, F. Plummer, A. Andonov, H. Artsob, N. Bastien, K. Bernard, T. F. Booth, D. Bowness, M. Czub, M. Drebot, L. Fernando, R. Flick, M. Garbutt, M. Gray, A. Grolla, S. Jones, H. Feldmann, A. Meyers, A. Kabani, Y. Li, S. Normand, U. Stroher, G. A. Tipples, S. Tyler, R. Vogrig, D. Ward, B. Watson, R. C. Brunham, M. Krajden, M. Petric, D. M. Skowronski, C. Upton, R. L. Roper, *Science* **2003**, *300 (5624)*, 1399–1404. DOI: 10.1126/science.1085953

[8] K. Anand, J. Ziebuhr, P. Wadhwani, J. R. Mesters, R. Hilgenfeld, *Science* **2003**, *300 (5626)*, 1763–1767. DOI: 10.1126/science.1085658

[9] K. C. Chou, D. Q. Wei, W. Z. Zhong, *Biochem. Biophys. Res. Commun.* **2003**, *308 (1)*, 148–151. DOI: 10.1016/S0006-291X(03)01342-1

[10] H. Yang, M. Yang, Y. Ding, Y. Liu, Z. Lou, Z. Zhou, L. Sun, L. Mo, S. Ye, H. Pang, G. F. Gao, K. Anand, M. Bartlam, R. Hilgenfeld, Z. Rao, *Proc. Natl. Acad. Sci. USA* **2003**, *100 (23)*, 13190–13195. DOI: 10.1073/pnas.1835675100

[11] Q. S. Du, S. Q. Wang, Y. Zhu, D. Q. Wei, H. Guo, S. Sirois, K. C. Chou, *Peptides* **2004**, *25 (11)*, 1857–1864. DOI: 10.1016/j.peptides.2004.06.018

[12] K. Fan, P. Wei, Q. Feng, S. Chen, C. Huang, L. Ma, B. Lai, J. Pei, Y. Liu, J. Chen, L. Lai, *J. Biol. Chem.* **2004**, *279 (3)*, 1637–1642. DOI: 10.1074/jbc.M310875200

[13] C. Huang, P. Wei, K. Fan, Y. Liu, L. Lai, *Biochemistry* **2004**, *43 (15)*, 4568–4574. DOI: 10.1021/bi036022q

[14] C. J. Kuo, Y. H. Chi, J. T. Hsu, P. H. Liang, *Biochem. Biophys. Res. Commun.* **2004**, *318 (4)*, 862–867. DOI: 10.1016/j.bbrc.2004.04.098

[15] J. E. Blanchard, N. H. Elowe, C. Huitema, P. D. Fortin, J. D. Cechetto, L. D. Eltis, E. D. Brown, *Chem. Biol.* **2004**, *11 (10)*, 1445–1453. DOI: 10.1016/j.chembiol.2004.08.011

[16] V. Graziano, W. J. McGrath, A. M. DeGruccio, J. J. Dunn, W. F. Mangel, *FEBS Lett.* **2006**, *580 (11)*, 2577–2583. DOI: 10.1016/j.febslet.2006.04.004

[17] K. Anand, G. J. Palm, J. R. Mesters, S. G. Siddell, J. Ziebuhr, R. Hilgenfeld, *EMBO J.* **2002**, *21 (13)*, 3213–3224. DOI: 10.1093/emboj/cdf327

[18] M. F. Hsu, C. J. Kuo, K. T. Chang, H. C. Chang, C. C. Chou, T. P. Ko, H. L. Shr, G. G. Chang, A. H. Wang, P. H. Liang, *J. Biol. Chem.* **2005**, *280 (35)*, 31257–31266. DOI: 10.1074/jbc.M502577200

[19] J. Shi, Z. Wei, J. Song, *J. Biol. Chem.* **2004**, *279 (23)*, 24765–24773. DOI: 10.1074/jbc.M311744200

[20] W. C. Hsu, H. C. Chang, C. Y. Chou, P. J. Tsai, P. I. Lin, G. G. Chang, *J. Biol. Chem.* **2005**, *280 (24)*, 22741–22748. DOI: 10.1074/jbc.M502556200

[21] C. Y. Chou, H. C. Chang, W. C. Hsu, T. Z. Lin, C. H. Lin, G. G. Chang, *Biochemistry* **2004**, *43 (47)*, 14958–14970. DOI: 10.1021/bi0490237

[22] J. Barrila, U. Bacha, E. Freire, *Biochemistry* **2006**, *45 (50)*, 14908–14916. DOI: 10.1021/bi0616302

[23] V. Graziano, W. J. McGrath, L. Yang, W. F. Mangel, *Biochemistry* **2006**, *45 (49)*, 14632–14641. DOI: 10.1021/bi061746y

[24] P. Wei, K. Fan, H. Chen, L. Ma, C. Huang, L. Tan, D. Xi, C. Li, Y. Liu, A. Cao, L. Lai, *Biochem. Biophys. Res. Commun.* **2006**, *339 (3)*, 865–872. DOI: 10.1016/j.bbrc.2005.11.102

[25] C. G. Wu, S. C. Cheng, S. C. Chen, J. Y. Li, Y. H. Fang, Y. H. Chen, C. Y. Chou, *Acta Crystallogr.* **2013**, *D69 (Pt 5)*, 747–755. DOI: 10.1107/S0907444913001315

[26] S. C. Cheng, G. G. Chang, C. Y. Chou, *Biophys. J.* **2010**, *98 (7)*, 1327–1336. DOI: 10.1016/j.bpj.2009.12.4272

[27] P. H. Liang, *Curr. Top. Med. Chem.* **2006**, *6 (4)*, 361–376. DOI: 10.2174/156802606776287090

[28] C. Y. Wu, J. T. Jan, S. H. Ma, C. J. Kuo, H. F. Juan, Y. S. Cheng, H. H. Hsu, H. C. Huang, D. Wu, A. Brik, F. S. Liang, R. S. Liu, J. M. Fang, S. T. Chen, P. H. Liang, C. H. Wong, *Proc. Natl. Acad. Sci. USA* **2004**, *101 (27)*, 10012–10017. DOI: 10.1073/pnas.0403596101

[29] A. Brik, Y. C. Lin, J. Elder, C. H. Wong, *Chem. Biol.* **2002**, *9 (8)*, 891–896. DOI: 10.1016/s1074-5521(02)00184-9

[30] K. S. Chan, S. T. Lai, C. M. Chu, E. Tsui, C. Y. Tam, M. M. Wong, M. W. Tse, T. L. Que, J. S. Peiris, J. Sung, V. C. Wong, K. Y. Yuen, *Hong Kong Med. J.* **2003**, *9 (6)*, 399–406.

[31] R. Y. Kao, W. H. Tsui, T. S. Lee, J. A. Tanner, R. M. Watt, J. D. Huang, L. Hu, G. Chen, Z. Chen, L. Zhang, T. He, K. H. Chan, H. Tse, A. P. To, L. W. Ng, B. C. Wong, H. W. Tsoi, D. Yang, D. D. Ho, K. Y. Yuen, *Chem. Biol.* **2004**, *11 (9)*, 1293–1299. DOI: 10.1016/j.chembiol.2004.07.013

[32] R. Y. Kao, A. P. To, L. W. Ng, W. H. Tsui, T. S. Lee, H. W. Tsoi, K. Y. Yuen, *FEBS Lett.* **2004**, *576 (3)*, 325–330. DOI: 10.1016/j.febslet.2004.09.026

[33] J. T. Hsu, C. J. Kuo, H. P. Hsieh, Y. C. Wang, K. K. Huang, C. P. Lin, P. F. Huang, X. Chen, P. H. Liang, *FEBS Lett.* **2004**, *574 (1–3)*, 116–120. DOI: 10.1016/j.febslet.2004.08.015

[34] R. C. Rowe, P. J. Sheskey, P. J. Weller, *Handbook of Pharmaceutical Excipients*, 4th ed., Pharmaceutical Press, Washington, DC, **2003**.

[35] Y. C. Liu, V. Huang, T. C. Chao, C. D. Hsiao, A. Lin, M. F. Chang, L. P. Chow, *Biochem. Biophys. Res. Commun.* **2005**, *333 (1)*, 194–199. DOI: 10.1016/j.bbrc.2005.05.095

[36] C. N. Chen, C. P. Lin, K. K. Huang, W. C. Chen, H. P. Hsieh, P. H. Liang, J. T. Hsu, *eCAM* **2005**, *2 (2)*, 209–215. DOI: 10.1093/ecam/neh081

[37] L. K. Leung, Y. Su, R. Chen, Z. Zhang, Y. Huang, Z. Y. Chen, *J. Nutr.* **2001**, *131 (9)*, 2248–2251.

[38] P. Hamill, D. Hudson, R. Y. Kao, P. Chow, M. Raj, H. Xu, M. J. Richer, F. Jean, *Biol. Chem.* **2006**, *387 (8)*, 1063–1074. DOI: 10.1515/BC.2006.131

[39] P. S. Dragovich, T. J. Prins, R. Zhou, S. E. Webber, J. T. Marakovits, S. A. Fuhrman, A. K. Patick, D. A. Matthews, C. A. Lee, C. E. Ford, B. J. Burke, P. A. Rejto, T. F. Hendrickson, T. Tuntland, E. L. Brown, J. W. Meador, 3rd, R. A. Ferre, J. E. Harr, M. B. Kosa, S. T. Worland, *J. Med. Chem.* **1999**, *42 (7)*, 1213–1224. DOI: 10.1021/jm9805384

[40] D. A. Matthews, P. S. Dragovich, S. E. Webber, S. A. Fuhrman, A. K. Patick, L. S. Zalman, T. F. Hendrickson, R. A. Love, T. J. Prins, J. T. Marakovits, R. Zhou, J. Tikhe, C. E. Ford, J. W. Meador, R. A. Ferre, E. L. Brown, S. L. Binford, M. A. Brothers, D. M. DeLisle, S. T. Worland, *Proc. Natl. Acad. Sci. USA* **1999**, *96 (20)*, 11000–11007. DOI: 10.1073/pnas.96.20.11000

[41] A. K. Patick, S. L. Binford, M. A. Brothers, R. L. Jackson, C. E. Ford, M. D. Diem, F. Maldonado, P. S. Dragovich, R. Zhou, T. J. Prins, S. A. Fuhrman, J. W. Meador, L. S. Zalman, D. A. Matthews, S. T. Worland, *Antimicrob. Agents Chemother.* **1999**, *43 (10)*, 2444–2450.

[42] M. He, R. Kania, J. Lou, S. Planken, *Patent US20060014821*, **2006**.

[43] R. S. Kania, L. J. Mitchell Jr, J. A. Nieman, *Patent WO2006061714*, **2006**.

[44] M. Bartlam, D. Ma, W. Xie, X. Xue, H. Yang, K. Yang, *Patent WO2006042478*, **2006**.

[45] H. Yang, W. Xie, X. Xue, K. Yang, J. Ma, W. Liang, Q. Zhao, Z. Zhou, D. Pei, J. Ziebuhr, R. Hilgenfeld, K. Y. Yuen, L. Wong, G. Gao, S. Chen, Z. Chen, D. Ma, M. Bartlam, Z. Rao, *PLoS Biol.* **2005**, *3 (10)*, e324. DOI: 10.1371/journal.pbio.0030324

[46] S. Yang, S. J. Chen, M. F. Hsu, J. D. Wu, C. T. Tseng, Y. F. Liu, H. C. Chen, C. W. Kuo, C. S. Wu, L. W. Chang, W. C. Chen, S. Y. Liao, T. Y. Chang, H. H. Hung, H. L. Shr, C. Y. Liu, Y. A. Huang, L. Y. Chang, J. C. Hsu, C. J. Peters, A. H. Wang, M. C. Hsu, *J. Med. Chem.* **2006**, *49 (16)*, 4971–4980. DOI: 10.1021/jm0603926

[47] J. J. Shie, J. M. Fang, T. H. Kuo, C. J. Kuo, P. H. Liang, H. J. Huang, Y. T. Wu, J. T. Jan, Y. S. Cheng, C. H. Wong, *Bioorg. Med. Chem.* **2005**, *13 (17)*, 5240–5252. DOI: 10.1016/j.bmc.2005.05.065

[48] J. J. Shie, J. M. Fang, C. J. Kuo, T. H. Kuo, P. H. Liang, H. J. Huang, W. B. Yang, C. H. Lin, J. L. Chen, Y. T. Wu, C. H. Wong, *J. Biol. Chem.* **2005**, *48 (13)*, 4469–4473. DOI: 10.1021/jm050184y

[49] R. P. Jain, H. I. Pettersson, J. Zhang, K. D. Aull, P. D. Fortin, C. Huitema, L. D. Eltis, J. C. Parrish, M. N. James, D. S. Wishart, J. C. Vederas, *J. Med. Chem.* **2004**, *47 (25)*, 6113–6116. DOI: 10.1021/jm0494873

[50] H. Z. Zhang, H. Zhang, W. Kemnitzer, B. Tseng, J. Cinatl, Jr., M. Michaelis, H. W. Doerr, S. X. Cai, *J. Med. Chem.* **2006**, *49 (3)*, 1198–1201. DOI: 1198-1201. 10.1021/jm0507678

[51] E. Martina, N. Stiefl, B. Degel, F. Schulz, A. Breuning, M. Schiller, R. Vicik, K. Baumann, J. Ziebuhr, T. Schirmeister, *Bioorg. Med. Chem. Lett.* **2005**, *15 (24)*, 5365–5369. DOI: 10.1016/j.bmcl.2005.09.012

[52] T. W. Lee, M. M. Cherney, C. Huitema, J. Liu, K. E. James, J. C. Powers, L. D. Eltis, M. N. James, *J. Mol. Biol.* **2005**, *353 (5)*, 1137–1151. DOI: 10.1016/j.jmb.2005.09.004

[53] S. Fuhrman, D. Matthews, A. Patick, P. Rejto, *Patent US20040235952*, **2004**.

[54] S. X. Cai, W. E. Kemnitzer, H. Z. Zhang, H. Zhang, *Patent WO2004101742*, **2005**.

[55] S. E. Webber, J. Tikhe, S. T. Worland, S. A. Fuhrman, T. F. Hendrickson, D. A. Matthews, R. A. Love, A. K. Patick, J. W. Meador, R. A. Ferre, E. L. Brown, D. M. DeLisle, C. E. Ford, S. L. Binford, *J. Med. Chem.* **1996**, *39 (26)*, 5072–5082. DOI: 10.1021/jm960603e

[56] L. R. Chen, Y. C. Wang, Y. W. Lin, S. Y. Chou, S. F. Chen, L. T. Liu, Y. T. Wu, C. J. Kuo, T. S. Chen, S. H. Juang, *Bioorg. Med. Chem. Lett.* **2005**, *15 (12)*, 3058–3062. DOI: 10.1016/j.bmcl.2005.04.027

[57] L. Zhou, Y. Liu, W. Zhang, P. Wei, C. Huang, J. Pei, Y. Yuan, L. Lai, *J. Med. Chem.* **2006**, *49 (12)*, 3440–3443. DOI: 10.1021/jm0602357

[58] X. Liu, J. Yang, A. M. Ghazi, T. K. Frey, *J. Virol.* **2000**, *74 (13)*, 5949–5956. DOI: 10.1128/JVI.74.13.5949-5956.2000

[59] T. D. Lockwood, *Arch. Biochem. Biophys.* **2004**, *432 (1)*, 12–24. DOI: 10.1016/j.abb.2004.09.011

[60] J. F. Petersen, M. M. Cherney, H. D. Liebig, T. Skern, E. Kuechler, M. N. James, *EMBO J.* **1999**, *18 (20)*, 5463–5475. DOI: 10.1093/emboj/18.20.5463

[61] G. J. Brewer, V. D. Johnson, R. D. Dick, P. Hedera, J. K. Fink, K. J. Kluin, *Hepatology* **2000**, *31 (2)*, 364–370. DOI: 10.1002/hep.510310216

[62] S. B. Mossad, *QJM* **2003**, *96 (1)*, 35–43. DOI: 10.1093/qjmed/hcg004

[63] B. D. Korant, J. C. Kauer, B. E. Butterworth, *Nature* **1974**, *248 (449)*, 588–590. DOI: 10.1038/248588a0

[64] V. J. Merluzzi, D. Cipriano, D. McNeil, V. Fuchs, C. Supeau, A. S. Rosenthal, J. W. Skiles, *Res. Commun. Chem. Pathol. Pharmacol.* **1989**, *66 (3)*, 425–440.

[65] U. Bacha, J. Barrila, A. Velazquez-Campoy, S. A. Leavitt, E. Freire, *Biochemistry* **2004**, *43 (17)*, 4906–4912. DOI: 10.1021/bi0361766

[66] E. Freire, R. Ottenbrite, Y. Xiao, A. Velazquez-Campoy, S. Leavitt, U. Bacha, J. Barrila, *Patent US20050267071*, **2006**.

[67] C. Y. Wu, K. Y. King, C. J. Kuo, J. M. Fang, Y. T. Wu, M. Y. Ho, C. L. Liao, J. J. Shie, P. H. Liang, C. H. Wong, *Chem. Biol.* **2006**, *13 (3)*, 261–268. DOI: 10.1016/j.chembiol.2005.12.008

[68] J. Balzarini, M. Preobrazhenskaya, E. De Clercq, *Patent US20050250677*, **2005**.

[69] I. L. Lu, N. Mahindroo, P. H. Liang, Y. H. Peng, C. J. Kuo, K. C. Tsai, H. P. Hsieh, Y. S. Chao, S. Y. Wu, *J. Med. Chem.* **2006**, *49 (17)*, 5154–5161. DOI: 10.1021/jm060207o

[70] S. Y. Wu, H. P. Hsieh, T. A. Hsu, I. L. Lu, *Patent US20060019967*, **2006**.

[71] K. C. Tsai, S. Y. Chen, P. H. Liang, I. L. Lu, N. Mahindroo, H. P. Hsieh, Y. S. Chao, L. Liu, D. Liu, W. Lien, T. H. Lin, S. Y. Wu, *J. Med. Chem.* **2006**, *49 (12)*, 3485–3495. DOI: 10.1021/jm050852f

[72] R. Rappuoli, V. Masignani, K. Stadler, J. Gregersen, D. Chien, J. Han, J. Polo, A. Weiner, M. Houghton, H. Song, M. Seo, J. Donnelly, H. Klenk, N. Valiante, *Patent US20060257852*, **2006**.

[73] L. Chen, C. Gui, X. Luo, Q. Yang, S. Gunther, E. Scandella, C. Drosten, D. Bai, X. He, B. Ludewig, J. Chen, H. Luo, Y. Yang, Y. Yang, J. Zou, V. Thiel, K. Chen, J. Shen, X. Shen, H. Jiang, *J. Virol.* **2005**, *79 (11)*, 7095–7103. DOI: 10.1128/JVI.79.11.7095-7103.2005

[74] J. Shen, H. Jiang, X. Shen, J. Zuo, X. Luo, D. Bai, J. Shen, K. Chen, C. Gui, L. Chen, J. Chen, Y. Yang, X. Zhuang, Y. Yang, X. He, H. Liu, B. Xiong, H. Luo, T. Sun, F. Ye, *Patent US20060142383*, **2006**.

[75] H. Jiang, X. Shen, J. Zuo, *Patent CN03129067*, **2006**.

[76] L. Lai, Y. Liu, K. Fan, Z. Liu, P. Wei, Q. Chen, J. Pei, S. Liu, *Patent CN03146047*, **2005**.

[77] J. Shen, H. Jiang, X. Shen, S. Li, W. Huang, C. Gui, J. Chen, T. Sun, F. Ye, D. Bai, H. Liu, X. Luo, K. Chen, *Patent CN200410018418*, **2005**.

[78] V. Thiel, K. A. Ivanov, A. Putics, T. Hertzig, B. Schelle, S. Bayer, B. Weissbrich, E. J. Snijder, H. Rabenau, H. W. Doerr, A. E. Gorbalenya, J. Ziebuhr, *J. Gen. Virol.* **2003**, *84 (Pt 9)*, 2305–2315. DOI: 10.1099/vir.0.19424-0

[79] A. C. Long, D. C. Orr, J. M. Cameron, B. M. Dunn, J. Kay, *FEBS Lett.* **1989**, *258 (1)*, 75–78. DOI: 10.1016/0014-5793(89)81619-9

[80] X. Xue, H. Yang, W. Shen, Q. Zhao, J. Li, K. Yang, C. Chen, Y. Jin, M. Bartlam, Z. Rao, *J. Mol. Biol.* **2007**, *366 (3)*, 965–975. DOI: 10.1016/j.jmb.2006.11.073

[81] C. J. Kuo, Y. P. Shih, D. Kan, P. H. Liang, *BioTechniques* **2009**, *47 (6)*, 1029–1032. DOI: 10.2144/000113303

[82] G. Zeng, *BioTechniques* **1998**, *25 (2)*, 206–208. DOI: 10.2144/000112297

[83] Y. P. Shih, W. M. Kung, J. C. Chen, C. H. Yeh, A. H. Wang, T. F. Wang, *Protein Sci.* **2002**, *11 (7)*, 1714–1719. DOI: 10.1110/ps.0205202

[84] H. M. Wang, Y. P. Shih, S. M. Hu, W. T. Lo, H. M. Lin, S. S. Ding, H. C. Liao, P. H. Liang, *Biotechnol. Prog.* **2009**, *25 (6)*, 1582–1586. DOI: 10.1002/btpr.274

[85] P. H. Liang, C. J. Kuo, Y. P. Shih, *Patent US20100203582*, **2010**.

[86] C. J. Kuo, H. G. Liu, Y. K. Lo, C. M. Seong, K. I. Lee, Y. S. Jung, P. H. Liang, *FEBS Lett.* **2009**, *583 (3)*, 549–555. DOI: 10.1016/j.febslet.2008.12.059

[87] C. C. Lee, C. J. Kuo, T. P. Ko, M. F. Hsu, Y. C. Tsui, S. C. Chang, S. Yang, S. J. Chen, H. C. Chen, M. C. Hsu, S. R. Shih, P. H. Liang, A. H. Wang, *J. Biol. Chem.* **2009**, *284 (12)*, 7646–7655. DOI: 10.1074/jbc.M807947200

[88] Z. Ren, L. Yang, N. Zhang, Y. Guo, C. Yang, Z. Luo, Z. Rao, *Protein Cell* **2013**, *4 (4)*, 248–250. DOI: 10.1007/s13238-013-2841-3

[89] A. K. Ghosh, G. Gong, V. Grum-Tokars, D. C. Mulhearn, S. C. Baker, M. Coughlin, B. S. Prabhakar, K. Sleeman, M. E. Johnson, A. D. Mesecar, *Bioorg. Med. Chem. Lett.* **2008**, *18 (20)*, 5684–5688. DOI: 10.1016/j.bmcl.2008.08.082

[90] A. Kilianski, A. M. Mielech, X. Deng, S. C. Baker, *J. Virol.* **2013**, *87 (21)*, 11955–11962. DOI: 10.1128/JVI.02105-13

